

Pyramid Hybrid Pooling Quantization for Efficient Fine-Grained Image Retrieval

Ziyun Zeng^{1*}, Jinpeng Wang^{1*}, Bin Chen^{2†}, Tao Dai³, Shu-Tao Xia¹

¹Tsinghua University ²Harbin Institute of Technology, Shenzhen, ³Shenzhen University
{zengzy21, wjp20}@mails.tsinghua.edu.cn, cb17@tsinghua.org.cn, daitao.edu@gmail.com, xiast@sz.tsinghua.edu.cn

Abstract

Deep hashing approaches, including deep quantization and deep binary hashing, have become a common solution to large-scale image retrieval due to high computation and storage efficiency. Most existing hashing methods can not produce satisfactory results for fine-grained retrieval, because they usually adopt the outputs of the last CNN layer to generate binary codes, which is less effective to capture subtle but discriminative visual details. To improve fine-grained image hashing, we propose **Pyramid Hybrid Pooling Quantization (PHPQ)**. Specifically, we propose a Pyramid Hybrid Pooling (PHP) module to capture and preserve fine-grained semantic information from multi-level features. Besides, we propose a learnable quantization module with a *partial* attention mechanism, which helps to optimize the most relevant codewords and improves the quantization. Comprehensive experiments demonstrate that PHPQ outperforms state-of-the-art methods.

Introduction

The explosively growing amount of images on the web raises the concern of search efficiency. Due to high efficiency in both computation and storage, hashing (Wang et al. 2015, 2017) has become a popular solution for large-scale retrieval. In general, the hashing methods can be categorized into two series, *i.e.*, binary hashing (Datar et al. 2004; Gong et al. 2012), and quantization (Jegou, Douze, and Schmid 2010; Ge et al. 2013). Binary hashing methods project high-dimensional data into short binary codes so that pairwise similarity can be quickly computed by Hamming distance. Quantization methods divide the origin feature space into disjoint subspaces and approximately represent the data points in each subspace by its centroid. By pre-computing a look-up table of inter-centroid similarities, the similarity between any data pair can be quickly obtained.

In the past few years, deep learning has become a common recipe for hashing methods. Note that most existing deep hashing methods (Liu et al. 2016; Yu et al. 2020) are designed for *coarse-grained* retrieval. They can only support image retrieval from general concepts, *e.g.* dogs or birds, which may fall short of practical needs. As a result, hashing for *fine-grained* retrieval becomes an important demand. Fine-grained image hashing requires discrimination among

sub-categories in a meta-category, such as different varieties of dogs. Therefore, it is more challenging to learn representations that keep robust to intra-class variances (*e.g.* various viewpoints and backgrounds) and discriminative to subtle inter-class differences. Unfortunately, coarse-grained hashing methods merely utilize the outputs of the last CNN feature layer to generate binary codes. They may lose visual details in images and produce inferior representations for fine-grained retrieval. On the other hand, recent fine-grained image hashing methods add heavy modules for region localization (Zeng, Lai, and Yin 2019; Ma et al. 2020) or local feature alignment (Cui et al. 2020). It is not surprising that these modules can help to capture fine-grained features, while they increase both memory and computation overhead. Besides, some of these methods require additional annotations such as bounding boxes, making it labor-intensive for application.

To improve the hashing for fine-grained image retrieval, we propose **Pyramid Hybrid Pooling Quantization (PHPQ)**. PHPQ is a quantization method that keeps more flexibility than binary hashing methods because larger cardinality of real space ensures greater representation capability than binary Hamming space (Cao et al. 2017a; Yuan et al. 2020). In PHPQ, we design a lightweight *Pyramid Hybrid Pooling (PHP) module* to extract multi-level semantic information, without additional annotations. The PHP module first utilizes pyramid features (Chen et al. 2018) from multiple CNN layers, each of which contains visual semantic information at a specific scale. Then, it fuses them through a tunable hybrid pooling strategy, which helps to focus and preserve critical semantic information from different visual scales. Besides, we propose a novel *partial codebook attention mechanism* to enhance quantization learning. Recently, Yu et al. (2020); Wang et al. (2021) applied the attention mechanism to relax *hard* (*i.e.*, nearest neighbor-based) codeword selection. The *soft* quantized representation for an image is the weighted sum of all codewords, where the attention weights are bounded and keep non-zero. Although the encoding process becomes differentiable, the optimization is less effective as *all* codewords, including those irrelevant ones, are updated in backpropagation. Since irrelevant codewords in the selection always receive perturbation, it degrades quantized representations and harms fine-grained retrieval. By contrast, our partial attention mechanism tries to filter out irrelevant codewords in the selection, guiding the optimization.

*Equal contribution.

†Corresponding author.

tion to those relevant ones attentively. Extensive experiments demonstrate that the partial attention mechanism improves deep quantization for fine-grained retrieval.

To summarize, we make the following contributions.

- We propose a deep quantization model for fine-grained image retrieval, which surpasses state-of-the-art methods.
- We propose a Pyramid Hybrid Pooling (PHP) module to capture and preserve fine-grained semantic information, which raises the discriminability of representations.
- We propose a *partial* codebook attention mechanism to improve learnable quantization. It can guide the optimization to relevant codewords attentively, leading to better quantized representations for fine-grained image retrieval.

Related Work

Deep Quantization Traditional quantization methods (Jegou, Douze, and Schmid 2010; Ge et al. 2013) directly adopt handcrafted features and achieve suboptimal performance. Recently, several deep quantization methods (Cao et al. 2016; Liu et al. 2018; Yu et al. 2020) with Convolutional Neural Networks (CNNs) (Krizhevsky, Sutskever, and Hinton 2012a; He et al. 2016) are proposed and achieve state-of-the-art performance. These works explore relational information among the training samples to learn semantic-preserved quantization. Nevertheless, they are designed for coarse-grained image retrieval tasks, leaving fine-grained quantization under-explored. Our PHPQ attempts to design a quantization scheme under the fine-grained scenario. Besides, we further investigate the issues in learnable quantization (Cao et al. 2016; Yu et al. 2020; Klein and Wolf 2017; Wang et al. 2021) and propose a novel partial attention mechanism to improve end-to-end quantization learning.

Fine-Grained Image Hashing In recent years, several deep hashing methods have been proposed to improve fine-grained image retrieval. For example, SRLH (Zeng, Lai, and Yin 2019) learns region localization and hash coding in a mutually reinforced way. CFH (Ma et al. 2020) utilizes the cross-modal correlation between semantic information and visual features to localize discriminative regions. ExchNet (Cui et al. 2020) aligns local features through a feature exchanging operation, producing discriminative part-level features while keeping the consistency of semantic information. Note that these methods rely on heavy sub-networks and thus increase the memory and computation overheads. Besides, some of them (*e.g.* ExchNet) require additional annotations for fine-grained visual localization, making it expensive for real-world applications. On the other hand, FPH (Yang et al. 2019) aggregates different pyramid feature maps from the convolution layers by average pooling, which keeps the efficiency. However, the average pooling is weak to extract fine-grained features, because it equally treats informative areas and noisy areas on the feature maps.

In contrast, PHPQ does not require additional annotations or heavy sub-networks. It extracts fine-grained features through a lightweight pyramid hybrid pooling module, where the pooling schemes are level-specific. Therefore, it can efficiently capture discriminative semantic information and generate better binary codes for fine-grained retrieval.

The Proposed Method

Problem Definition

Given a labeled training set $\{(\mathbf{I}_n, y_n)\}_{n=0}^{N-1}$, where $\mathbf{I}_n \in \mathbb{R}^P$ denotes the P -dimensional flattened image vector and $y_n \in \{0, 1, \dots, N_c - 1\}$ denotes the fine-grained category label for this image. The goal of quantization is to learn a quantizer $q : \mathbb{R}^P \mapsto \{0, 1\}^B$ that maps the raw image vector \mathbf{I}_n to a binary code $\mathbf{b}_n \in \{0, 1\}^B$ that preserves semantic information. To this end, we propose **Pyramid Hybrid Pooling Quantization (PHPQ)**, which can be trained in an end-to-end manner. Figure 1 illustrates the framework of PHPQ. We describe the details in the following sections.

Pyramid Hybrid Pooling Module

Generalized Spatial Pooling Spatial pooling (Wang and Shang 2006) is an efficient way to produce powerful descriptors from the convolutional feature maps. There are two representative methods in spatial pooling, *i.e.*, the Global Maximum Pooling (GMP) (Tolias, Sirci, and Jégou 2015) and the Global Average Pooling (GAP) (Babenko and Lempitsky 2015). However, neither of them is powerful enough to capture discriminative fine-grained details, because: (i) GMP focuses on the highest response elements in the feature map while ignoring other small but discriminative regions to fine-grained recognition. (ii) GAP equally treats all feature map areas, which produces less discriminative descriptors with noisy information from the background.

To address the shortcomings, Generalized Spatial Pooling (GSP) (Radenović, Tolias, and Chum 2018) compromises between GMP and GAP to capture discriminative details while reducing the noise. Given an input image \mathbf{I} , the feature map produced by one convolutional layer is denoted as $\mathbf{F} \in \mathbb{R}^{H \times W \times C}$, where $\mathbf{F}^i \in \mathbb{R}^{H \times W}$, $i = 1, 2, \dots, C$, is the tensor of the i -th channel. Let a_ρ^i be the pooled output of i -th channel and $\mathbf{f} \in \mathbb{R}^C$ be the descriptor generated by GSP, then we have

$$a_\rho^i = \frac{1}{HW} \left(\sum_{h \in H} \sum_{w \in W} \mathbf{F}_{hw}^i{}^\rho \right)^{\frac{1}{\rho}}, \quad (1)$$

$$\mathbf{f} = \text{GSP}_\rho(\mathbf{F}) = [a_\rho^0, a_\rho^1, \dots, a_\rho^{C-1}], \quad (2)$$

where ρ is the focus factor of GSP. Note that when $\rho = 1$, GSP is equivalent to GAP and acts as GMP when $\rho \rightarrow +\infty$. A larger ρ leads to smaller high-response areas.

To better understand how GSP works, we analyze the gradient of pooled output a_ρ^i w.r.t. \mathbf{F}_{hw}^i :

$$\frac{\partial a_\rho^i}{\partial \mathbf{F}_{hw}^i} = \frac{1}{HW} \left(\sum_{h' \in H} \sum_{w' \in W} \mathbf{F}_{h'w'}^i{}^\rho \right)^{\frac{1}{\rho}-1} \cdot \mathbf{F}_{hw}^i{}^{\rho-1}, \quad (3)$$

As shown in Eq.(3), with a fixed \mathbf{F}_{hw}^i , the gradients grow exponentially as ρ increases. A larger ρ can highlight high response areas that contain discriminative parts and in the meantime restrain the gradients to low response areas such as the background. Hence by selecting a proper ρ , GSP can capture various discriminative details simultaneously while filtering out noises.

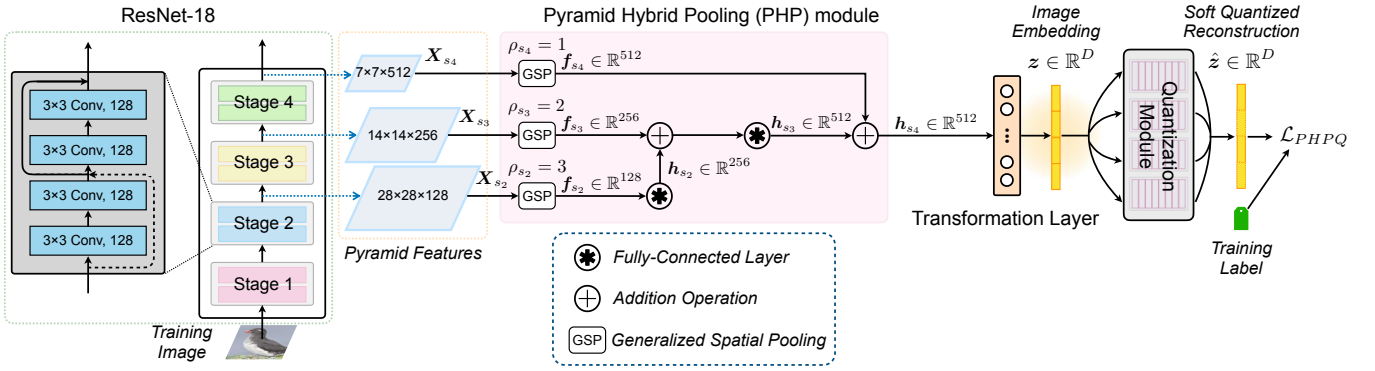


Figure 1: The training framework of the **Pyramid Hybrid Pooling Quantization (PHPQ)**. First, we send the raw image into a standard CNN, *e.g.* ResNet-18, and extract pyramid features from different stages. Then, we aggregate these multi-level features by the proposed Pyramid Hybrid Pooling (PHP) module and get the image embedding through a transformation layer. Next, the image embedding will be quantized and reconstructed through the quantization module, where we propose a partial attention mechanism to enhance end-to-end quantization learning. Finally, we define a learning objective with the soft quantized reconstructed embedding and optimize the model by back-propagation.

Hybrid Pooling CNNs naturally provide multi-scale features because of their inherent pyramidal structures. To take advantage of such features, we propose a Pyramid Hybrid Pooling (PHP) module. Specifically, we first extract the feature maps from the i -th stage of a ResNet-18 as X_{s_i} , $i \in \{2, 3, 4\}$, respectively. Then, we apply GSP with different focus factors $\{\rho_{s_i}\}_{i=2}^4$ to X_{s_i} , $i \in \{2, 3, 4\}$, respectively:

$$f_{s_i} = \text{GSP}_{\rho_{s_i}}(X_{s_i}), i \in \{2, 3, 4\}, \quad (4)$$

Empirically, the feature maps at lower stages contain information of visual details while the feature maps at higher stages contain abstract semantic information. We control the focus factors $\{\rho_{s_i}\}_{i=2}^4$ to satisfy $\rho_{s_i} > \rho_{s_{i-1}}$ such that the model can capture fine-grained discriminative details in shallow layers while preserving high-level semantic information in deeper layers.

Next, we fuse multi-level GSP descriptors by

$$h_{s_2} = \text{FC}(f_{s_2}), \quad (5)$$

$$h_{s_3} = \text{FC}(h_{s_2} + f_{s_3}), \quad (6)$$

$$h_{s_4} = h_{s_3} + f_{s_4}, \quad (7)$$

where FC denotes a fully connected layer without activation. Finally, we apply a transformation layer $g: \mathbb{R}^{D_{s_4}} \mapsto \mathbb{R}^D$ for the linear fused representation h_{s_4} and get the image embedding:

$$z = g(h_{s_4}) \in \mathbb{R}^D. \quad (8)$$

Quantization Module

Product Quantization and Soft Quantization Product quantization (Jegou, Douze, and Schmid 2010) has been widely applied in large-scale retrieval systems (Johnson, Douze, and Jégou 2019). Given an image embedding $z \in \mathbb{R}^D$, we first split it into M equal-length sub-vectors, *i.e.*, $z = [z_0, z_1, \dots, z_{M-1}]$, $z_m \in \mathbb{R}^d$, $d = D/M$. Then we quantize these sub-vectors by vector quantization independently. For the m -th sub-vector, traditional vector quantization assigns the codeword to the input vector by clustering:

$$q_m(z_m) = c_m^{k^*}, \text{ s.t. } k^* = \arg \min_k \|z_m - c_m^k\|_2, \quad (9)$$

where $q_m(\cdot)$ represents the sub-vector quantizer for the m -th sub-vector and $c_m^k \in \mathbb{R}^d$ denotes the k -th sub-codewords in m -th sub-codebook, $C_m \in \mathbb{R}^{K \times d}$. The whole codebook is derived from the cartesian product of the M sub-codebooks, *i.e.*, $C = C_0 \times \dots \times C_{M-1}$. In this way, the embedding space can be divided into K^M disjoint cells and the embeddings in each cell can be represented by the cell centroid. Hence, the pairwise distance (similarity) can be approximated measured by the inter-centroid distance (similarity).

Note that such a clustering-based step can not be trained by back-propagation, so it is hard to be integrated into the deep learning framework. To tackle this issue, we adopt the soft quantization scheme proposed in (Yu et al. 2020). Firstly, we apply ℓ_2 normalization to all codewords and sub-vectors:

$$c_m^k \leftarrow c_m^k / \|c_m^k\|_2, \quad z_m \leftarrow z_m / \|z_m\|_2. \quad (10)$$

Then we calculate the attention scores on each sub-codebook:

$$p_m = [p_m^0, p_m^1, \dots, p_m^{K-1}] \in \mathbb{R}^K, \quad (11)$$

$$p_m^k = \frac{e^{2\alpha \langle z_m, c_m^k \rangle}}{\sum_{k'=0}^{K-1} e^{2\alpha \langle z_m, c_m^{k'} \rangle}}, m \in \{0, 1, \dots, M-1\}, \quad (12)$$

where $\langle \cdot, \cdot \rangle$ denotes the inner-product, α is a scaling factor.

Next, we aggregate the sub-codewords in each sub-codebook according to the codebook attention scores:

$$\hat{z}_m = p_m C_m = \sum_{k=0}^{K-1} p_m^k c_m^k. \quad (13)$$

Finally, the soft quantized reconstruction embedding \hat{z} *w.r.t.* the original image embedding z is concatenated by

$$\hat{z} = [\hat{z}_0, \hat{z}_1, \dots, \hat{z}_{M-1}]. \quad (14)$$

Since the softmax operator is differentiable, the soft quantization is learnable by the back-propagation.

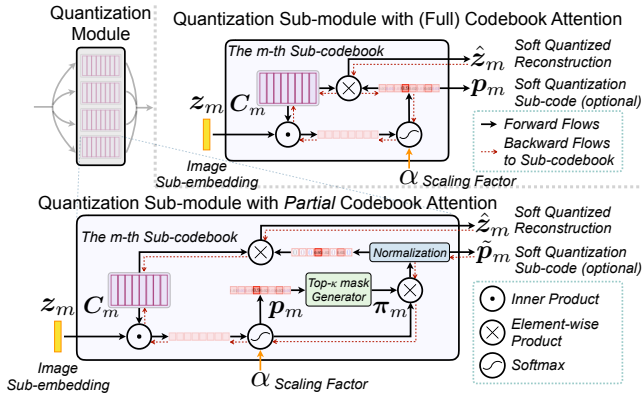


Figure 2: The learnable quantization module with the *partial* attention mechanism in PHPQ. In the m -th quantization sub-module, we generate a mask π_m for the sub-embedding z_m by ranking all the attention scores in p_m . Then we use the mask to select the top- κ entries in p_m and disable the rest entries. Finally, we get the soft assigned codeword for z_m by partial attentive pooling with the C_m and the masked attention scores \tilde{p}_m .

Partial Attention for Soft Quantization Although the soft quantization mechanism enables learnable quantization, it leads to a gap between soft quantization in the training stage and hard quantization in the inference stage. To mitigate this gap, existing methods (Yu et al. 2020; Klein and Wolf 2017; Wang et al. 2021) adopt a large α in the codebook attention and make the attention scores approximate to the one-hot distribution. However, simply enlarging α will increase the difficulty of updating codeword selection, and the quantization model may be trapped in sub-optimal solutions. On the other hand, a smaller α helps to optimize the model, but it fails to exclude irrelevant codewords, *i.e.*, the codewords that are associated with the least attention weights. Since the attention weights for irrelevant codewords keep non-zero, these codewords will contribute to the soft quantized representations (Eq.(13)) and also be updated in backpropagation. Hence, irrelevant codewords will always be perturbed by the “noisy” gradients, which degrade quantization and harm fine-grained retrieval.

To improve such issues, we propose a *partial* attention mechanism to improve learnable quantization, as shown in Figure 2. First, we sort all the attention scores derived from Eq.(12) in descending order and collect the indexes of the codewords associated with the top- κ attention scores, where κ is a threshold hyper-parameter. We denote the collected top- κ index set as $\mathcal{I}_{\text{top-}\kappa}$. Then, we generate an attention mask $\pi_m = [\pi_m^0, \pi_m^1, \dots, \pi_m^{K-1}]$ for the i -th sub-codebook:

$$\pi_m^k = \begin{cases} 1, & k \in \mathcal{I}_{\text{top-}\kappa} \\ 0, & \text{otherwise} \end{cases}, \quad k \in \{0, 1, \dots, K-1\}. \quad (15)$$

Next, we multiply π_m with the origin weight vector p_m to disable the irrelevant scores:

$$p_m \leftarrow p_m \otimes \pi_m, \quad (16)$$

where \otimes denotes element-wise product operation.

After that, we normalize p_m and get refined scores \tilde{p}_m by

$$\tilde{p}_m^k = p_m^k / \left(\sum_{k'=0}^{K-1} p_m^{k'} \right). \quad (17)$$

Finally, we rewrite Eq.(13) as

$$\hat{z}_m = \tilde{p}_m C_m = \sum_{k=0}^{K-1} \tilde{p}_m^k c_m^k. \quad (18)$$

By Eq.(15)-(18), only codewords that share top- κ similarity with origin data will be considered, while others are regarded as irrelevant ones and will be ignored. From another point of view, partial attention acts as a filter and removes redundant noise (*e.g.* the wrong class information) contained in irrelevant codewords, therefore helps to retain the fine-grained discriminative features during soft reconstruction.

Loss Function

We follow Zeng, Lai, and Yin (2019) and apply a Soft Reconstruction-based Cross-Entropy Loss (SR-CEL) to train the model, namely,

$$\mathcal{L}_{\text{SR-CEL}} = \frac{1}{N} \sum_{n=0}^{N-1} \left(-\log \frac{e^{o_{ny_n}/\tau}}{\sum_{c'=0}^{N_c-1} e^{o_{nc'}/\tau}} \right) \quad (19)$$

where N , N_c represent the mini-batch size and the number of categories respectively, o_{nc} denotes the logit of the classifier that the n -th image belongs to the c -th category, y_n is the ground-truth label for the n -th image, and τ denotes the temperature hyper-parameter for the classifier.

Besides, to learn compact intra-class representations and discriminative inter-class representations, we adopt the Contrastive Loss (CL) (Hadsell, Chopra, and LeCun 2006), namely,

$$d^+ = \frac{1}{|\mathcal{B}_c|^2} \sum_{\hat{z} \in \mathcal{B}_c} \sum_{\hat{z}^+ \in \mathcal{B}_c \setminus \{\hat{z}\}} \|\hat{z} - \hat{z}^+\|_2, \quad (20)$$

$$d^- = \frac{1}{|\mathcal{B}_c|(|\mathcal{B}| - |\mathcal{B}_c|)} \sum_{\hat{z} \in \mathcal{B}_c} \sum_{\hat{z}^- \in \mathcal{B} \setminus \mathcal{B}_c} \|\hat{z} - \hat{z}^-\|_2, \quad (21)$$

$$\mathcal{L}_{\text{CL}} = \max(d^+ - m^+, 0) + \max(m^- - d^-, 0), \quad (22)$$

where \mathcal{B} denotes the set of soft quantized reconstructions for the images in the current training mini-batch, \mathcal{B}_c denotes a specific subset of \mathcal{B} that is associated with the c -th category. m^+ and m^- are the pre-defined positive and negative margins respectively.

Therefore, the overall loss function of PHPQ is

$$\mathcal{L}_{\text{PHPQ}} = \mathcal{L}_{\text{SR-CEL}} + \gamma \mathcal{L}_{\text{CL}}, \quad (23)$$

where γ is a hyper-parameter to balance two loss terms.

Encoding and Retrieval

In the inference, the database images are encoded into a series of codeword indexes through hard quantization. Given an image I , we first obtain the image embedding $z =$

$[z_0, \dots, z_{M-1}]$. The semantic index $i = [i_0, \dots, i_{M-1}]$ is computed by searching the nearest codewords:

$$i_m = \arg \max_k \langle z_m, c_m^k \rangle, \quad k \in \{0, 1, \dots, K-1\}. \quad (24)$$

In Eq.(24), each i only takes $M \log_2 K$ bits to be stored, which implies the high storage efficiency of quantization.

As for retrieval, we use Asymmetric Quantizer Distance (AQD) (Jegou, Douze, and Schmid 2010). Given a query I^q and a database item I^d , AQD computes their similarity by:

$$\text{AQD}(I^q, I^d) = \sum_{m=0}^{M-1} \langle v_m^q, c_m^{i_m^d} \rangle. \quad (25)$$

To accelerate similarity computation, we can pre-compute a query-to-codeword lookup table. Concretely, we define $\Xi_m^q \in \mathbb{R}^{M \times K}$ as the lookup table for m -th sub-codebook, in which $\Xi_m^{q, i_m^d} = \langle v_m^q, c_m^{i_m^d} \rangle$. After obtaining Ξ_m^q , we can compute the similarity by summing up M look-up entries:

$$\text{AQD}(I^q, I^d) = \sum_{m=0}^{M-1} \Xi_m^{q, i_m^d}. \quad (26)$$

Experiments and Results

Experimental Setup

Datasets We conduct experiments on two fine-grained benchmarks: **(i) CUB-200-2011** (Wah et al. 2011) is a fine-grained bird dataset, which consists of 11,788 images belonging to 200 categories. The training set contains 5,994 images while the test set contains the rest 5,794 images. The reference database is identical to the training set. **(ii) Stanford Dogs** (Khosla et al. 2011) is a fine-grained dog dataset consisting of 20,580 images in 120 categories. There are about 150 images per category. 100 images are picked per category to form the training set, while the rest 8,580 images are used as the test set. We adopt the official split strategy in (Yang et al. 2019; Zeng, Lai, and Yin 2019), and take the respective training set as the reference database.

Evaluation Metrics Two metrics in previous works (Jegou, Douze, and Schmid 2010; Cui et al. 2020; Zeng, Lai, and Yin 2019; Yang et al. 2019; Cao et al. 2017b) are adopted to measure the performance of the proposed PHPQ, *i.e.*, the Mean Average Precision (**MAP**), and the Precision curves *w.r.t.* different numbers of top returned items (**P@N**). The MAP is defined as:

$$\text{MAP} = \frac{1}{Q} \sum_{i=0}^{Q-1} \frac{1}{N_{\text{rel}(i)}} \sum_{n=0}^{N_D-1} \frac{N_{\text{rel}(i)}^n}{n} \cdot \mathbb{I}(k), \quad (27)$$

where Q denotes the total number of queries, N_D denotes the database size, $N_{\text{rel}(i)}$ denotes the total number of relevant items *w.r.t.* the i -th query, $N_{\text{rel}(i)}^n$ represents the number of relevant images in top- n returned results. $\mathbb{I}(k)$ is an indicator function, which is equal to 1 once the k -th returned image shares the same category with the query, otherwise $\mathbb{I}(k) = 0$.

Baselines We compare the PHPQ with 15 generic baselines: **(i)** 11 coarse-grained hashing methods, LSH (Datar et al. 2004), SH (Weiss et al. 2008), PQ (Jegou, Douze, and Schmid 2010), ITQ (Gong et al. 2012), OPQ (Ge et al. 2013), DPSH (Li, Wang, and Kang 2015), DTH (Lai et al. 2015), DSH (Liu et al. 2016), HashNet (Cao et al. 2017b), ADSh (Jiang and Li 2018), and PQN (Yu et al. 2020). **(ii)** 4 fine-grained hashing methods, FPH (Yang et al. 2019), SRLH (Zeng, Lai, and Yin 2019), ExchNet (Cui et al. 2020), and CFH (Ma et al. 2020).

Implementation Details The proposed PHPQ is implemented with PyTorch (Paszke et al. 2019) and the experiments are conducted on a GeForce RTX 2080 Ti GPU. We adopt a ResNet-18 (He et al. 2016) pre-trained on ImageNet (Krizhevsky, Sutskever, and Hinton 2012b) as the backbone. The maximum training epoch is set to be 70 with batch size 64. We adopt Adam (Kingma and Ba 2015) as the optimizer. The initial learning rate is set to be 0.0001. Other hyper-parameters are listed as follows: **(i)** The focus factor of GSP, $\rho_{s_2} = 3$, $\rho_{s_3} = 2$, and $\rho_{s_4} = 1$. **(ii)** The embedding dimension, $D = 1536$. **(iii)** The size of a sub-codebook, $K = 256$, while the number of codebook M varies in $\{2, 4, 6, 8\}$ such that each code takes $M \log_2 K$ bits. **(iv)** The scaling factor for soft quantization, $\alpha = 16$. **(v)** The temperature parameter for \mathcal{L}_{SR-CEL} , $\tau = 0.50$ for CUB-200-2011, and $\tau = 0.25$ for Stanford Dogs. **(vi)** The weight parameters for \mathcal{L}_{PHPQ} , $\gamma = 1$.

Results and Analysis

Results We report the MAP results in Table 1, which shows that our PHPQ outperforms all comparison baselines. Specifically, compared to CFH, the best baseline, PHPQ achieves an average MAP increase of **3.33%** and **1.73%** on CUB-200-2011 and Stanford Dogs respectively. PHPQ with partial attention mechanism can optimize the codebook more effectively in quantization learning. Therefore, it produces better binary codes for fine-grained image retrieval and performs better than state-of-the-art quantization methods, *e.g.* PQ, OPQ, and PQN. Furthermore, compared with CFH and SRLH, the performance gap of PHPQ between the two datasets is smaller. It indicates that the proposed PHP module improves the generalization ability to capture fine-grained features among different types of objects.

Figure 3 shows the Precision curves of top N returned items (**P@N**) on CUB-200-2011 and Stanford Dogs under 16 bits. PHPQ consistently finds more relevant images in the top- N ($N < 100$) returned list, which is favorable because the users may pay more attention to the top-ranked results in a retrieval system.

Component Analysis To explore the contribution of each component, we design 6 variants of PHPQ: **(i)** PHPQ_{last fc} directly adopts the outputs of the last fully connected layer of ResNet-18 as image features. **(ii)** PHPQ_{GAP} adopts global average pooling in the PHP module, *i.e.*, setting $\rho_{s_1} = \rho_{s_2} = \rho_{s_3} = 1$ in Eq.(4). **(iii)** PHPQ_{GMP} adopts global maximum pooling in the PHP module, *i.e.*, setting $\rho_{s_1} = \rho_{s_2} = \rho_{s_3} = +\infty$ in Eq.(4). **(iv)** PHPQ _{$\rho_{s_1} < \rho_{s_2} < \rho_{s_3}$} adopts $\rho_{s_1} < \rho_{s_2} < \rho_{s_3}$ in the PHP module. We set

Table 1: Mean Average Precision (MAP) results of different models under different bits on CUB-200-2011 and Stanford Dogs.

Method	CUB-200-2011				Stanford Dogs			
	16 bits	32 bits	48 bits	64 bits	16 bits	32 bits	48 bits	64 bits
LSH (Datar et al. 2004)	8.67	9.14	18.57	19.31	8.01	19.54	30.99	41.62
SH (Weiss et al. 2008)	26.39	43.90	51.39	55.12	25.26	43.69	49.69	55.66
PQ (Jegou, Douze, and Schmid 2010)	35.01	41.95	52.16	54.94	43.64	44.42	47.32	48.45
ITQ (Gong et al. 2012)	25.19	45.96	53.76	58.97	31.70	46.59	54.37	57.40
OPQ (Ge et al. 2013)	34.89	43.68	52.90	55.09	39.97	52.65	51.75	52.07
DPSH (Li, Wang, and Kang 2015)	34.97	43.01	49.08	52.25	42.70	55.28	60.80	62.31
DTH (Lai et al. 2015)	46.41	54.54	57.71	58.81	54.35	62.58	63.62	65.73
DSH (Liu et al. 2016)	31.56	49.30	54.08	59.67	47.28	55.87	61.28	63.19
HashNet (Cao et al. 2017b)	37.91	46.28	48.53	51.23	47.45	55.21	55.75	59.34
ADSH (Jiang and Li 2018)	42.93	57.65	67.19	72.28	47.91	61.05	66.38	68.60
PQN (Yu et al. 2020)	59.07	65.89	70.39	72.91	65.94	67.04	70.76	70.95
FPH (Yang et al. 2019)	51.69	58.32	61.24	62.33	63.40	69.09	70.60	71.30
SRLH (Zeng, Lai, and Yin 2019)	69.08	69.22	70.87	70.10	66.68	74.02	75.16	75.38
ExchNet (Cui et al. 2020)	-	67.74	71.05	-	-	-	-	-
CFH (Ma et al. 2020)	72.08	73.41	73.21	72.71	79.33	79.96	79.47	79.34
PHPQ_(Ours)	76.03	76.24	76.25	76.21	81.01	81.27	81.44	81.29

Table 2: The MAP results for different PHPQ variants under different bits on CUB-200-2011 and Stanford Dogs.

Variant	CUB-200-2011				Stanford Dogs			
	16 bits	32 bits	48 bits	64 bits	16 bits	32 bits	48 bits	64 bits
PHPQ	76.03	76.24	76.25	76.21	81.01	81.27	81.44	81.29
PHPQ _{last fc}	74.13 (-1.90)	74.54 (-1.70)	74.61 (-1.64)	74.72 (-1.49)	79.83 (-1.18)	80.14 (-1.13)	80.32 (-1.12)	80.26 (-1.03)
PHPQ _{GAP}	75.35 (-0.68)	75.65 (-0.59)	75.80 (-0.45)	75.64 (-0.57)	80.81 (-0.20)	80.94 (-0.33)	80.83 (-0.61)	80.52 (-0.77)
PHPQ _{GMP}	73.70 (-2.33)	74.14 (-2.10)	74.30 (-1.95)	74.12 (-2.09)	79.57 (-1.44)	79.93 (-1.34)	80.06 (-1.38)	79.80 (-1.49)
PHPQ _{$\rho_{s_1} < \rho_{s_2} < \rho_{s_3}$}	75.15 (-0.88)	75.52 (-0.72)	75.54 (-0.71)	75.36 (-0.85)	80.11 (-0.90)	80.53 (-0.74)	80.70 (-0.74)	80.40 (-0.89)
PHPQ _{full attn}	75.03 (-1.00)	75.74 (-0.50)	75.99 (-0.26)	75.98 (-0.23)	80.38 (-0.63)	80.42 (-0.85)	80.67 (-0.77)	80.45 (-0.84)
PHPQ _{w/o \mathcal{L}_{CL}}	73.30 (-2.73)	74.25 (-1.99)	74.69 (-1.56)	74.48 (-1.73)	78.07 (-2.94)	77.98 (-3.29)	77.88 (-3.56)	77.56 (-3.73)

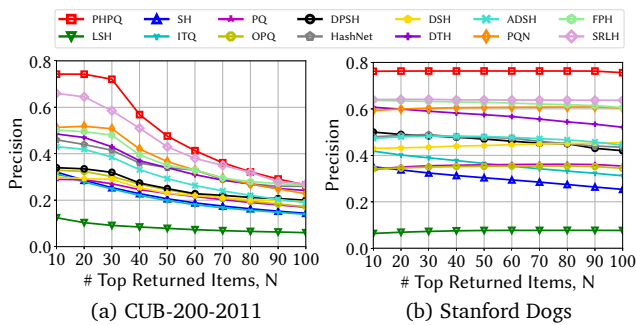


Figure 3: Precision@top- N curves under 16 bits on CUB-200-2011 and Stanford Dogs.

$\rho_{s_1} = 1, \rho_{s_2} = 2, \rho_{s_3} = 3$ in Eq.(4) for this variant. (v) PHPQ_{full attn} removes the partial attention mechanism in the quantization module by setting $\kappa = 256$ in Eq.(15). (vi) PHPQ_{w/o \mathcal{L}_{CL}} removes \mathcal{L}_{CL} in Eq.(23) and uses \mathcal{L}_{SR-CEL} as the loss function. According to the results in Table 2, we can learn the following conclusions.

The PHP module helps to capture and preserve multi-level visual features. PHPQ outperforms PHPQ_{last fc} by an average MAP of 1.68% and 1.12% on CUB-200-2011 and Stanford Dogs. It implies that the last FC layer of CNN is ineffective to capture fine-grained discriminative features, thus is not enough to be applied in fine-grained scenarios. Besides, PHPQ also outperforms PHPQ_{GMP} and PHPQ_{GAP}. The reason can be explained by two-folds: (i) GMP has a relatively small activated area. It pays most attention to the highest response element, while missing other discriminative clues for fine-grained retrieval. (ii) GAP treats each element in a feature map equally. It fails to filter out noisy information from the background, thus producing less discriminative descriptors for fine-grained quantization. By contrast, the proposed PHP module shows superior performance to capture fine-grained semantic information, thus contributing to better quantized representations. Moreover, PHPQ outperforms PHPQ _{$\rho_{s_1} < \rho_{s_2} < \rho_{s_3}$} . It indicates that a descending order of focus factors helps to make the best of PHP module because a larger ρ helps to capture visual details in lower stages while a small ρ can better preserve high-level semantic information in higher stages.

Table 3: The MAP results *w.r.t.* different attention threshold κ s under different bits on CUB-200-2011 and Stanford Dogs.

κ	CUB-200-2011				Stanford Dogs			
	16 bits	32 bits	48 bits	64 bits	16 bits	32 bits	48 bits	64 bits
1	67.41	73.47	74.51	75.03	50.56	74.76	77.91	79.55
5	76.03	76.24	76.25	76.21	81.01	81.27	81.44	81.29
25	75.87	75.98	76.15	76.12	80.79	80.97	81.23	81.05
125	75.14	75.82	76.03	76.03	80.53	80.54	80.87	80.59
256	75.03	75.74	75.99	75.98	80.38	80.42	80.67	80.45

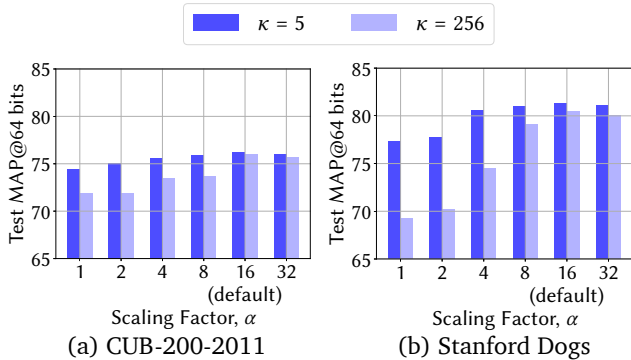


Figure 4: The MAP results with partial attention ($\kappa = 5$) and full attention ($\kappa = K = 256$) *w.r.t.* different scaling factors in soft quantization. The models are evaluated under 64 bits.

Partial attention improves the quantization learning. PHPQ performs better than PHPQ_{full attn} on all settings, especially at low-bit representations. Note that the scaling factor α is also an important factor in quantization training, we further investigate the relation between α and the partial attention mechanism. As shown in Figure 4, the partial attention can consistently improve the quantization learning under different α s, which indicates that partial attention can be a universal way to improve trainable quantization. Besides, the large α also makes the model more difficult to be optimized and converge. By contrast, with the help of partial attention, the model can achieve comparable performance with the best one even α is relatively small. As a result, the training efficiency is boosted without losing much precision.

We also explore the selection of the partial attention threshold κ . As shown in Table 3, the model performs best under $\kappa = 5$. A tight threshold increases the risk of missing relevant codewords in the optimization. For example, the model performance under $\kappa = 1$ is not satisfactory. On the other side, a loose threshold is not favorable either, because it reduce the filtering effect of partial attention. For instance, when $\kappa = K = 256$, the model achieves suboptimal performance compared with other settings, *i.e.*, $\kappa = 5, 25, 125$.

Contrastive loss helps to learn discriminative quantization representation. PHPQ outperforms PHPQ_{w/o \mathcal{L}_{CL}} . It shows that \mathcal{L}_{CL} plays an assistant role to improve the intra-class compactness and inter-class diversity, thus making the classification borders clearer and improving retrieval performance.

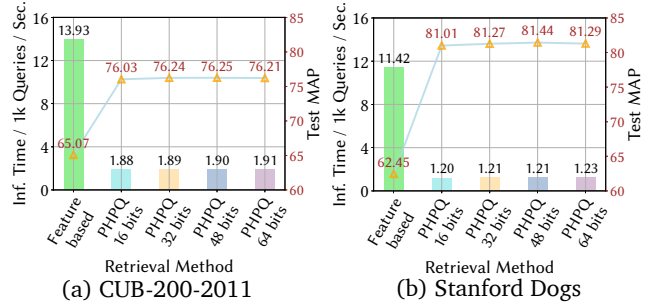


Figure 5: The average inference time per 1×10^3 queries in seconds and the MAP results of different retrieval methods on CUB-200-2011 and Stanford Dogs.

Efficiency Analysis Figure 5 shows the inference time of different retrieval methods *w.r.t.* 1×10^3 queries in seconds and their MAP results on two datasets. The average speed of PHPQ is **7.35** and **9.41** times faster than feature-based retrieval on CUB-200-2011 and Stanford Dogs respectively, which demonstrates the efficiency of our approach. Interestingly, we find a similar phenomenon as Yu et al. (2020) that the quantization-based methods even produce better retrieval results than the original feature-based method. The reason is that quantization acts as an additional regularization on the outputs, thus suppresses overfitting (Yu et al. 2020).

Conclusions

In this paper, we propose a deep quantization model for fine-grained image retrieval, namely Pyramid Hybrid Pooling Quantization (PHPQ). Concretely, we propose a Pyramid Hybrid Pooling (PHP) module that captures and preserves fine-grained semantic information through generalized spatial pooling over multi-level features. Besides, we propose a learnable quantization module with a *partial* attention mechanism, which helps to optimize the most relevant codewords and improves the performance. Comprehensive experiments demonstrate the superiority of PHPQ over state-of-the-art baselines. The future work is two-fold: (i) An input-aware or class-aware pooling scheme for the PHP module. (ii) A dynamic partial attention mechanism that adapts the number of candidate codewords during the training.

Table 4: The MAP results of PHPQ *w.r.t.* different soft quantization scaling factor α in Eq.(12) on CUB-200-2011 and Stanford Dogs with different number of bits.

α	CUB-200-2011				Stanford Dogs			
	16bits	32bits	48bits	64bits	16bits	32bits	48bits	64bits
1	71.86	75.80	77.02	77.42	64.95	72.73	75.96	77.37
2	73.83	77.17	77.96	78.09	69.56	74.93	76.59	77.74
4	77.86	78.36	78.58	78.55	80.25	80.99	81.00	80.54
8	78.72	79.19	79.18	78.93	80.43	81.19	81.46	80.99
16	79.03	79.24	79.25	79.21	81.01	81.27	81.44	81.29
32	78.84	78.97	79.04	79.01	80.73	81.15	81.22	81.13

Appendix

Additional Experiments

The Sensitivity of α The MAP *w.r.t.* various soft quantization scaling factor α on CUB-200-2011 and Stanford Dogs are reported in Table 4. We can infer that neither the largest nor the smallest α in soft quantization achieve the best performance. This can be explained by the fact that when $\alpha \rightarrow 1$, the excessive soft reconstruction varies drastically from hard reconstruction during the testing phase. On the other hand, as $\alpha \rightarrow +\infty$, the soft assignment operation is equivalent to the $\arg \max$ function. In this case, the gradients of those non-prominent codewords tend to vanish, making the optimization more difficult. In result, the model achieves inferior performance. Based on the above results, we set $\alpha = 16$ in default for both of the two datasets.

The Sensitivity of τ Table 5 reports the MAP *w.r.t.* different temperature parameter τ in \mathcal{L}_{SR-CEL} on CUB-200-2011 and Stanford Dogs. A larger τ makes the model less confident, thus avoids overfitting and increases the correction capability. On the other hand, a smaller τ improves the optimization efficiency and helps to converge.

In fine-grained image retrieval, the correction capability is crucial, as the model is easily misled by the confusing appearance of different fine-grained classes. Therefore, it's important to choose a reasonable setting of τ . According to Table 5, we set $\tau = 0.50$ and $\tau = 0.25$ for CUB-200-2011 and Stanford Dogs respectively.

Visualization To show the superiority of the proposed PHPQ intuitively, we illustrate the top-10 retrieved items returned by PHPQ and the state-of-the-art deep quantization approach, *i.e.*, PQN, on CUB-200-2011 and Stanford Dogs respectively in Figure 6. It's clear to see that the relevance of the top-10 ranked images returned by PHPQ is higher than that of PQN, which implies PHPQ is more user-friendly and practical under real scenarios.

References

Babenko, A.; and Lempitsky, V. 2015. Aggregating local deep features for image retrieval. In *Proceedings of the IEEE international conference on computer vision*, 1269–1277.

Cao, Y.; Long, M.; Wang, J.; and Liu, S. 2017a. Deep visual-semantic quantization for efficient image retrieval. In *Proceedings of the IEEE Conference on Computer Vision and Pattern Recognition*, 1328–1337.

Table 5: The MAP results of PHPQ *w.r.t.* different temperature parameter τ in \mathcal{L}_{SR-CEL} (Eq.(19)) on CUB-200-2011 and Stanford Dogs with different number of bits.

τ	CUB-200-2011				Stanford Dogs			
	16bits	32bits	48bits	64bits	16bits	32bits	48bits	64bits
0.25	78.51	78.94	79.02	78.61	81.01	81.27	81.44	81.29
0.50	79.03	79.24	79.25	79.21	80.42	80.73	80.96	80.96
0.75	77.75	79.11	79.09	79.25	80.32	80.68	80.84	80.81
1.00	78.02	78.89	78.83	78.95	80.12	80.75	80.82	80.74

Query	Top-10 Retrieved Items										
CUB-200-2011											PHPQ P@10 90%
Least Auklet											PQN P@10 80%
Stanford Dogs											PHPQ P@10 100%
Irish Terrier											PQN P@10 80%

Figure 6: The top-10 images returned by PHPQ and PQN under 64 bits on CUB-200-2011 and Stanford Dogs.

Cao, Y.; Long, M.; Wang, J.; Zhu, H.; and Wen, Q. 2016. Deep quantization network for efficient image retrieval. In *Proceedings of the AAAI Conference on Artificial Intelligence*, volume 30.

Cao, Z.; Long, M.; Wang, J.; and Yu, P. S. 2017b. Hashnet: Deep learning to hash by continuation. In *Proceedings of the IEEE international conference on computer vision*, 5608–5617.

Chen, Y.; Wang, Z.; Peng, Y.; Zhang, Z.; Yu, G.; and Sun, J. 2018. Cascaded pyramid network for multi-person pose estimation. In *Proceedings of the IEEE conference on computer vision and pattern recognition*, 7103–7112.

Cui, Q.; Jiang, Q.-Y.; Wei, X.-S.; Li, W.-J.; and Yoshie, O. 2020. ExchNet: A Unified Hashing Network for Large-Scale Fine-Grained Image Retrieval. In *European Conference on Computer Vision*, 189–205. Springer.

Datar, M.; Immorlica, N.; Indyk, P.; and Mirrokni, V. S. 2004. Locality-sensitive hashing scheme based on p-stable distributions. In *Proceedings of the twentieth annual symposium on Computational geometry*, 253–262.

Ge, T.; He, K.; Ke, Q.; and Sun, J. 2013. Optimized product quantization for approximate nearest neighbor search. In *Proceedings of the IEEE Conference on Computer Vision and Pattern Recognition*, 2946–2953.

Gong, Y.; Lazebnik, S.; Gordo, A.; and Perronnin, F. 2012. Iterative quantization: A procrustean approach to learning binary codes for large-scale image retrieval. *IEEE transactions on pattern analysis and machine intelligence*, 35(12): 2916–2929.

Hadsell, R.; Chopra, S.; and LeCun, Y. 2006. Dimensionality reduction by learning an invariant mapping. In *2006 IEEE Computer Society Conference on Computer Vision*

- and *Pattern Recognition (CVPR'06)*, volume 2, 1735–1742. IEEE.
- He, K.; Zhang, X.; Ren, S.; and Sun, J. 2016. Deep residual learning for image recognition. In *Proceedings of the IEEE conference on computer vision and pattern recognition*, 770–778.
- Jégou, H.; Douze, M.; and Schmid, C. 2010. Product quantization for nearest neighbor search. *IEEE transactions on pattern analysis and machine intelligence*, 33(1): 117–128.
- Jiang, Q.-Y.; and Li, W.-J. 2018. Asymmetric deep supervised hashing. In *Proceedings of the AAAI Conference on Artificial Intelligence*, volume 32.
- Johnson, J.; Douze, M.; and Jégou, H. 2019. Billion-scale similarity search with GPUs. *IEEE Transactions on Big Data*, 1–1.
- Khosla, A.; Jayadevaprakash, N.; Yao, B.; and Li, F.-F. 2011. Novel dataset for fine-grained image categorization: Stanford dogs. In *Proc. CVPR Workshop on Fine-Grained Visual Categorization (FGVC)*, volume 2. Citeseer.
- Kingma, D. P.; and Ba, J. 2015. Adam: A Method for Stochastic Optimization. In *ICLR (Poster)*.
- Klein, B.; and Wolf, L. 2017. In defense of product quantization. *arXiv preprint arXiv:1711.08589*, 2(3): 4.
- Krizhevsky, A.; Sutskever, I.; and Hinton, G. E. 2012a. Imagenet classification with deep convolutional neural networks. *Advances in neural information processing systems*, 25: 1097–1105.
- Krizhevsky, A.; Sutskever, I.; and Hinton, G. E. 2012b. Imagenet classification with deep convolutional neural networks. *Advances in neural information processing systems*, 25: 1097–1105.
- Lai, H.; Pan, Y.; Liu, Y.; and Yan, S. 2015. Simultaneous feature learning and hash coding with deep neural networks. In *Proceedings of the IEEE conference on computer vision and pattern recognition*, 3270–3278.
- Li, W.-J.; Wang, S.; and Kang, W.-C. 2015. Feature learning based deep supervised hashing with pairwise labels. *arXiv preprint arXiv:1511.03855*.
- Liu, B.; Cao, Y.; Long, M.; Wang, J.; and Wang, J. 2018. Deep triplet quantization. In *Proceedings of the 26th ACM international conference on Multimedia*, 755–763.
- Liu, H.; Wang, R.; Shan, S.; and Chen, X. 2016. Deep supervised hashing for fast image retrieval. In *Proceedings of the IEEE conference on computer vision and pattern recognition*, 2064–2072.
- Ma, L.; Li, X.; Shi, Y.; Wu, J.; and Zhang, Y. 2020. Correlation filtering-based hashing for fine-grained image retrieval. *IEEE Signal Processing Letters*, 27: 2129–2133.
- Paszke, A.; Gross, S.; Massa, F.; Lerer, A.; Bradbury, J.; Chanan, G.; Killeen, T.; Lin, Z.; Gimelshein, N.; Antiga, L.; et al. 2019. PyTorch: An Imperative Style, High-Performance Deep Learning Library. *Advances in Neural Information Processing Systems*, 32: 8026–8037.
- Radenović, F.; Tolias, G.; and Chum, O. 2018. Fine-tuning CNN image retrieval with no human annotation. *IEEE transactions on pattern analysis and machine intelligence*, 41(7): 1655–1668.
- Tolias, G.; Sicre, R.; and Jégou, H. 2015. Particular object retrieval with integral max-pooling of CNN activations. *arXiv preprint arXiv:1511.05879*.
- Wah, C.; Branson, S.; Welinder, P.; Perona, P.; and Belongie, S. 2011. The Caltech-UCSD Birds-200-2011 Dataset. Technical Report CNS-TR-2011-001, California Institute of Technology.
- Wang, J.; Chen, B.; Dai, T.; and Xia, S.-T. 2021. Webly Supervised Deep Attentive Quantization. In *ICASSP 2021 - 2021 IEEE International Conference on Acoustics, Speech and Signal Processing (ICASSP)*, 2250–2254.
- Wang, J.; Liu, W.; Kumar, S.; and Chang, S.-F. 2015. Learning to hash for indexing big data—A survey. *Proceedings of the IEEE*, 104(1): 34–57.
- Wang, J.; Zhang, T.; Sebe, N.; Shen, H. T.; et al. 2017. A survey on learning to hash. *IEEE transactions on pattern analysis and machine intelligence*, 40(4): 769–790.
- Wang, Z.; and Shang, X. 2006. Spatial pooling strategies for perceptual image quality assessment. In *2006 International Conference on Image Processing*, 2945–2948. IEEE.
- Weiss, Y.; Torralba, A.; Fergus, R.; et al. 2008. Spectral hashing. In *Nips*, volume 1, 4. Citeseer.
- Yang, Y.; Geng, L.; Lai, H.; Pan, Y.; and Yin, J. 2019. Feature pyramid hashing. In *Proceedings of the 2019 on International Conference on Multimedia Retrieval*, 114–122.
- Yu, T.; Meng, J.; Fang, C.; Jin, H.; and Yuan, J. 2020. Product Quantization Network for Fast Visual Search. *International Journal of Computer Vision*, 128(8): 2325–2343.
- Yuan, L.; Wang, T.; Zhang, X.; Tay, F. E.; Jie, Z.; Liu, W.; and Feng, J. 2020. Central similarity quantization for efficient image and video retrieval. In *Proceedings of the IEEE/CVF Conference on Computer Vision and Pattern Recognition*, 3083–3092.
- Zeng, H.; Lai, H.; and Yin, J. 2019. Simultaneous region localization and hash coding for fine-grained image retrieval. *arXiv preprint arXiv:1911.08028*.